THE JOURNAL OF PHYSICAL CHEMISTRY C

Article

pubs.acs.org/JPCC

Three-Dimensional Electrochemical Lithography in Mesoporous TiO_2 Thin Films

M. M. Linares Moreau,[†,‡] L. P. Granja,[*,†] M. C. Fuertes,[‡,§] E. D. Martínez,[∥] V. Ferrari,[†,‡] P. E. Levy,[†] and G. J. A. A. Soler-Illia[§,⊥]

[†]Departamento de Física de la Materia Condensada, Gerencia de Investigación y Aplicaciones, Centro Atómico Constituyentes, Comisión Nacional de Energía Atómica, Av. Gral. Paz 1499, 1650, San Martín, Buenos Aires, Argentina

[‡]Instituto Sabato, Universidad Nacional de General San Martín, Centro Atómico Constituyentes, Comisión Nacional de Energía Atómica,, 1650, San Martín, Buenos Aires, Argentina

[§]Gerencia de Química, Centro Atómico Constituyentes, Comisión Nacional de Energía Atómica, Av. Gral. Paz 1499, 1650, San Martín, Buenos Aires, Argentina

[∥]Laboratorio de Bajas Temperaturas-Instituto de Nanociencia y Nanotecnología (INN), Gerencia de Física, Centro Atómico Bariloche, Comisión Nacional de Energía Atómica, Av. Bustillo 9500, 8400, S. C. de Bariloche, Río Negro Argentina

[⊥]Instituto de Nanosistemas, Universidad Nacional de General San Martín, Av. 25 de Mayo y Francia, 1650, San Martín, Buenos Aires, Argentina

Supporting Information

ABSTRACT: Electrochemical processes at water−titania interfaces in TiO_2 thin films were studied using conducting-tip atomic force microscopy. Mesoporous titania thin films were prepared by sol−gel synthesis from molecular precursors with the addition of surfactants to induce the formation of a porous structure. We found that both three-dimensional local resistance and topography are significantly and irreversibly changed in the submicrometer range by applying a constant bias voltage, with water playing a fundamental role in this process. The mesoporous structure enhances these effects due to the highly water accessible porous titania surface, which can be easily tuned by changing the synthesis procedure. Our findings are important in the development and performance of titania-based electronic microdevices and could pave the way toward the design of new electrochemical lithography methods.

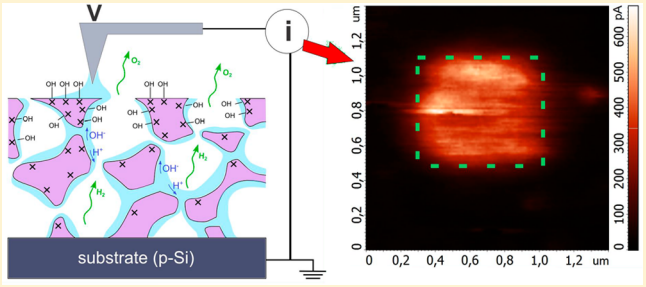

INTRODUCTION

Titanium dioxide has attracted wide interest over decades due to its great variety of physical properties with actual and potential applications in catalysis, solar cells, protective coatings, gas sensors, and electronic devices.[1] Within this scenario, surface science has focused its interest in understanding, improving, and exploiting the surface and interface properties of titania, where oxygen atoms (or equivalently oxygen vacancies) play a fundamental role.[2] Oxygen vacancies are also key for the photocatalytic behavior of titania in water molecules dissociation.[3] Regarding applications in electronic devices, TiO_2 has become a prototypical memristive material[4] whose characteristics arise directly from the electrode metal−oxide interface, and the mechanisms involved are mainly electrochemical, electrothermal/thermochemical, pure electronic, and structural transformations. Moreover, the electric response of TiO_2 is strongly dependent on the fabrication technique, i.e., the sample morphology (crystallinity, grain boundaries, defects, microporosity, stoichiometry, etc.),[4] and it is well-known that the porosity, and more specifically the accessible porosity, is critical for the physical properties of TiO_2 films.[5,6] However, microporosity and the interaction with environmental parameters, such as humidity and atmospheric pressure, have not yet been seriously considered as sources of the lack of reproducibility during the electronic device performance testing.

In the last decades, great progress has been made on developing new nanofabrication techniques based on scanning probe microscopies (SPM).[7] Within this framework, redox tip−sample interactions have prompted the study of the electrochemical processes occurring at the tip−sample interface. In particular, when SPM experiments are performed in ambient conditions, these redox processes are usually mediated by a water meniscus.[8] These studies gave rise to an electrochemical lithography (EL) whose peculiar characteristic is the use of the substrate as the reactive layer to "write" through the thickness of the film.[9,10] As a result, localized changes in the physical properties can be patterned within a homogeneous medium

Received: September 27, 2015
Revised: November 27, 2015
Published: December 2, 2015

DOI: 10.1021/acs.jpcc.5b09418
J. Phys. Chem. C 2015, 119, 28954−28960

without morphological modifications. In this way, EL emerges as a candidate for the so-called "third way" for nanofabrication, previously proposed for multifunctional oxides.[11]

In the case of titania, electrical and electrochemical surface properties have already been studied using several SPM techniques.[12−14] In particular, for conducting-tip atomic force microscopy (CAFM) experiments carried out in O_2 atmosphere, local resistance increment, and topographic protrusions were reported when positive bias voltage was applied to the tip. To explain these results, the authors propose that non stoichiometric TiO_2 transforms to the stoichiometric insulating state by oxygen absorption at the surface.[13,15]

Mesoporous oxides, obtained using a combination of the sol−gel method and the self-assembly of surfactants, are materials with a high surface area, controlled porosity, and an ordered array of pores that can be tuned in the 2−20 nm diameter range.[16] When these materials are processed as thin films, they present a variety of applications, ranging from sensors to supercapacitors and biodevices.[17] The quality of the mesoporous films, which present a very low rugosity, makes them ideal to be incorporated in microdevice fabrication. Moreover, the pores can be filled with different species (solvents, organic molecules, nanoparticles, etc.) in order to tune the properties of the materials.[18] When TiO_2 mesoporous films deposited on silicon substrates are thermally treated at temperatures higher than 300 °C, they present anatase nanocrystalline structure. Thus, TiO_2 mesoporous thin films are particularly interesting because they combine the properties of titania-based materials with a very accessible and controlled pore structure.[19]

In this work, we present CAFM experiments performed in controlled environmental relative humidity (RH) conditions on mesoporous TiO_2 (MT) thin films. Test experiments were also carried out in non-mesoporous TiO_2 (NMT) and mesoporous SiO_2 (MS) thin films. In the case of the MT films, we found that the electric conduction can be locally increased in an area scanned with an applied bias voltage. This effect possibly involves a titania-mediated water electrolysis along with a superficially reduced TiO_2. Interestingly, we observed that the film topography is also modified for high RH values, suggesting that some products of the water electrolysis might be adsorbed at the reduced titania surface. The mesoporous structure was exploited to enhance the local electrochemical processes at the water−titania interfaces. In this way, combining CAFM with the mesoporous structure, we were able to change the inner electrical properties of the film at the submicrometric scale, inspiring new tridimensional EL methods in a simple alternative way to the traditional top-down or bottom-up approaches for device fabrication.

EXPERIMENTAL METHODS

Synthesis of Sol−Gel Thin Films. Mesoporous oxide thin films were synthesized following the sol−gel route in combination with the evaporation induced self assembly strategy (EISA).[15] For the case of mesoporous TiO_2, Pluronic F127 was added to an ethanolic solution of $TiCl_4$ (Merck), and then water was incorporated to promote hydrolysis of the Ti precursor. The molar ratio $TiCl_4$/F127/H_2O/EtOH used was 1:0.005:10:40. The solution was heated up to 32 °C and was dip coated at a withdrawal speed of 1.0 mm·s^{-1} in a humidity controlled environment of 35% RH. Non-mesoporous titania films were made in the same way but in the absence of surfactants and deposited at 40 °C in dry conditions (∼20% RH). SiO_2 mesoporous films were synthesized using tetraethoxysilane (TEOS, Merck) as the oxide precursor and F127 as template; the solution molar ratio TEOS/F127/H_2O/EtOH used was 1:0.005:10(HCl 0.004):40. This solution was aged for 24 h before the film deposition on the substrate to obtain an ordered mesopores structure.

In all cases, silicon p-type (boron-doped) was used as substrate, and after deposition the films were kept for 24 h in a chamber at 50% RH, to promote stabilization of the mesostructure, then submitted to 60 °C for 24 h, 130 °C for 24 h, and finally calcined at 350 °C for 2 h.[20] This thermal treatment ensures the complete removal of the F127 surfactant.[21,22] After this treatment, the films were washed with acetone and immersed for 2 h in an ethanol/water 1:1 v/v mixture under strong agitation in order to remove any residue from the surfactant decomposition. The films were finally dried at 130 °C.

After the thermal treatment at 350 °C, NMT films could retain some porosity due to the sol−gel process. An additional thermal treatment at 650 °C during 15 min was performed to reduce this porosity and obtain a more dense material.[5]

Materials Characterization. Ellipsometric porosimetry (EP), 2D-SAXS, and electron microscopy were used to structurally characterize the thin films. Water adsorption−desorption isotherms (at 25 °C) were measured by EP (SOPRA GES5A). This experimental technique is very powerful for micro- and mesopores characterization of supported porous thin films.[23,24] The experimental device is based on the coupling of a pressure controlled chamber and a spectroscopic ellipsometer. Film thickness and refractive index values are obtained from the ellipsometric parameters Ψ and Δ under nitrogen flux containing variable water vapor quantities; P/P_0 is varied from 0 to 1 (P_0 being the saturation water vapor at 25 °C and P the vapor pressure measured). Water volume adsorbed at each P/P_0 value is determined by modeling the refractive index obtained according to a three component (water−air−oxide) effective medium approximation. Adsorption−desorption isotherms are then plotted using the water volume adsorbed by the porous film at each P/P_0. Modeling these results, it is also possible to obtain the pores sizes distribution (PSD) of the mesostructure.

CAFM images were acquired with a Solver Pro NT-MDT Scanning Probe Microscope. Electric current and topography were simultaneously scanned with a Pt coated Si tip in contact mode. Scans were performed applying a constant bias voltage (V) between the nanoscale tip (curvature radio ca. 35 nm) and the sample substrate[25] with $V = \pm 10$ V. The silicon substrate was contacted with silver paint to a conductive sample holder electrically grounded. The relative humidity was monitored and controlled by applying a soft dry air flow over the sample inside the microscope chamber. All the CAFM experiments were carried out for RH < 50% in order to avoid water condensation on the sample surface that would affect the AFM performance.

RESULTS AND DISCUSSION

The porous accessibility and the mesostructure of our films were characterized by EP. Figure 1 compares the water adsorption−desorption isotherms of the MT, MS, and NMT films. Capillary condensation occurs first in the MS film for RH values between 60% and 70% and second in the MT for RH between 65% and 80%. In both cases there is a residual microporosity (due to the sol−gel process) that is full of adsorbed water at low RH values before the occurrence of the

DOI: 10.1021/acs.jpcc.5b09418
J. Phys. Chem. C 2015, 119, 28954−28960

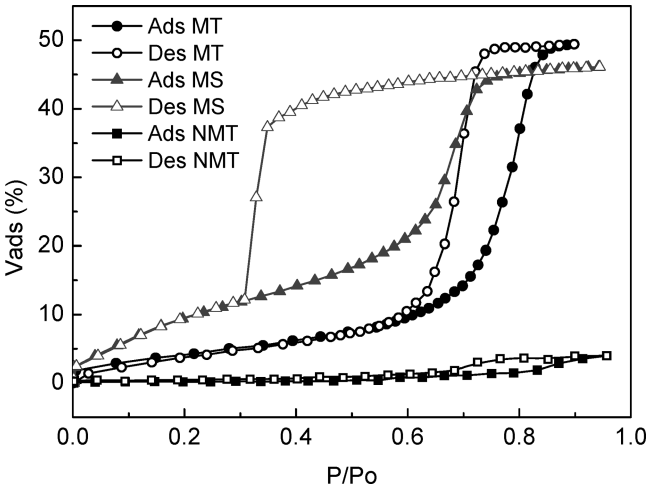

Figure 1. Water adsorption−desorption isotherms (V_{ads} is the percentage of the porous volume filled with water, P_0 is the saturation water vapor at 25 °C, and P is the vapor pressure measured) of a mesoporous TiO_2 (MT), a mesoporous SiO_2 (MS), and a non-porous TiO_2 (NMT) films. Full and open symbols denote the adsorption branches and desorption branches, respectively.

capillary condensation. The NMT film has a very low porosity due to the flash thermal treatment at high temperatures, and pores have very little amount of adsorbed water for RH values lower than 70%. Table 1 summarizes the structural character-

Table 1. Structural Data of the Mesoporous and Non-porous Titania (MT and NMT) and Mesoporous Silica (MS) Thin Films[a]

film	porosity (%)	D_{pores} (nm)	D_{necks} (nm)	thickness (nm)
MT	49 ± 5	8.7 ± 0.5	5.7 ± 0.5	150 ± 10
NMT	4.0 ± 0.5	-----	-----	34 ± 3
MS	46 ± 5	6.5 ± 0.5	2.3 ± 0.2	90 + 5

[a]Results obtained using ellipsometric porosimetry. Pores and necks diameters (D_{pores} and D_{necks}, respectively) extracted from the pores sizes distribution (PSD) are displayed for the mesoporous films (see SI for more detailed structural information).

ization obtained from EP for the MT, NMT, and MS films. Note that the water porous accessibility is about 50% for both mesoporous films in contrast with 4% for NMT. The structural information for MT and MS is complemented with 2D-SAXS, from which it can be calculated that the mesopore structure is contracted nearly 50% in the direction perpendicular to the substrate and that the periodic arrangement of pores resembles a cubic *Im*3*m* structure. (More details about the structural characterization of the films are presented at the SI.)

In the following, we address the effects of the humidity on the surface properties of the mesoporous TiO_2 film using CAFM. We focus our study on the changes in the conduction and the topography of the scanned area by applying a bias voltage in different controlled environmental humidity conditions. Regarding the electric behavior, we observed that the magnitude of the current increases with RH for $V > 0$, while no current was measured for $V < 0$, independently of RH. We identified three regimes depending on the environmental conditions: RH > 40%, 30% < RH < 40%, and RH < 30%.

The typical behavior obtained for RH > 40% is shown in Figure 2. Initially, a square region of 500 nm × 500 nm was scanned with an applied voltage of either −10 V or +10 V. In both cases, this procedure was followed by a second scan with +10 V into a larger area of 1.4 μm × 1.4 μm. The electric current images (Figure 2b,d) show that there is a reduction of the local resistance in the previously scanned region of 500 nm × 500 nm. Regarding topography, only the area where a positive voltage was applied is modified (Figure 2c), while in the negative bias case, it remains the same (Figure 2a).

In the intermediate RH regime, no surface modification was found when several consecutive areas were scanned in different bias voltage conditions (Figure 3a,c). However, the conduction enhancement effect is still present for both polarities. It is remarkable that it is not possible to erase the conduction effect alternating the electric polarities (Figure 3d). Even more, the conduction increases with the successive scans, as can be seen in Figure 3b,d. The effect is irreversible and remains for several hours after being performed. When measuring with −10 V, the modified conductive region cannot be distinguished due to the low current level observed. (The effects of alternating V or using different V for writing and reading actions, as well as the spatial resolution and time evolution of the patterns, are shown in detail in the SI).

For RH < 30% there was no measurable current during the CAFM scan for the bias voltage range explored (shown at SI). Consequently, neither topography nor conductive effects appear.

Control experiments were carried out on mesoporous SiO_2 and non-mesoporous TiO_2 films (details in the SI). Neither of these samples exhibit traces of the successive scans at the topography and current images. For NMT, the magnitude of the current increases with the relative humidity for RH > 30% and $V > 0$, but electric conduction disappears after drying off the air inside the AFM chamber, and no current was measured for $V < 0$, independently of the RH conditions. In the MS case, no electric conduction was obtained for all RH and voltage conditions considered.

In the case of MT and NMT films, the presence of a Schottky barrier for the Pt−TiO_2 interface at the tip−sample contact[26] has to be considered. This rectifier junction is forward polarized when a positive bias is applied, allowing electrons to flow from the TiO_2 film into the tip. Under a reverse bias voltage, when the tip is negatively polarized, the electron transport is strongly reduced. The CAFM results described above are consistent with the non-linear and asymmetric current−voltage response expected for the mentioned Schottky barrier (see SI, for current−voltage curves and further discussion). A considerable tip−sample contact resistance appears as a consequence of this barrier, and the bias voltage is effectively applied to the series resistance of the tip−sample contact and the film thickness. As a result, the real voltage drop at the film is lower than the nominal bias voltage during the experiment, so an applied voltage above 6 V is necessary to obtain an electric current flow through the MT film (see SI).

In order to discuss the possible mechanisms involved in the CAFM results for the MT films, we have considered three main parallel conduction channels contributing to the electric current between the tip and the substrate: (i) the TiO_2 film itself where the conduction mainly develops through oxygen vacancies and defects, (ii) the water layer adsorbed on the TiO_2 pores connecting the surface of the film with the Si substrate, and (iii) the water−TiO_2 interface inside the pores.

On one hand, our results show that the electric properties are strongly dependent on both the environmental humidity and

DOI: 10.1021/acs.jpcc.5b09418
J. Phys. Chem. C 2015, 119, 28954−28960

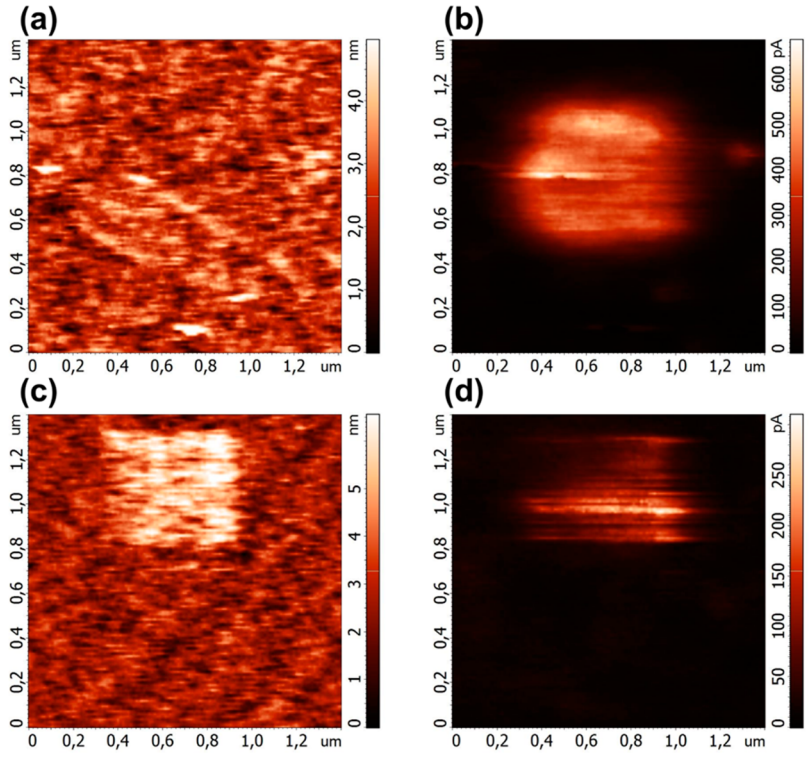

Figure 2. Topographic (left) and electric current (right) images of a mesoporous TiO_2 film in a 1.4 μm × 1.4 μm area for 50% RH and a constant bias of 10 V, where a 500 nm × 500 nm area had been previously scanned applying either −10 V (a,b) and +10 V (c,d).

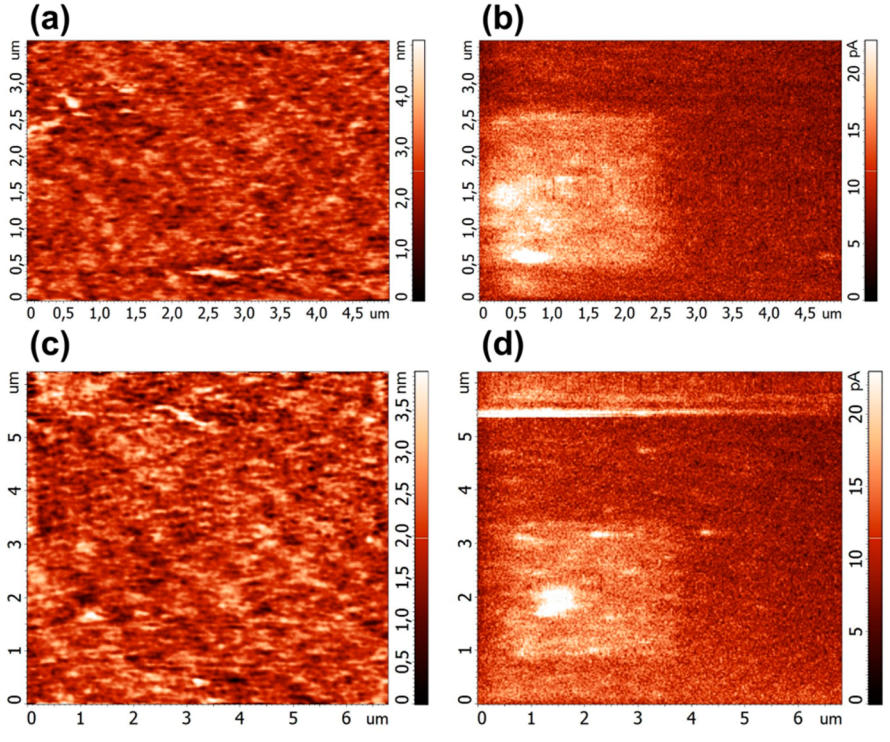

Figure 3. Topographic (left) and current (right) images of a mesoporous TiO_2 film for 38% RH. (a,b) First, a 500 nm × 500 nm area was scanned; second, the scanning area was enlarged to 2 μm × 2 μm, and third, to 5 μm × 5 μm. For the three cases +10 V bias voltage was applied while scanning. (c,d) First, a 500 nm × 500 nm area was scanned with −10 V, followed by a 3 μm × 3 μm applying +10 V, then by a 5 μm × 5 μm with −10 V, and finally by a 7 μm × 7 μm applying +10 V.

the porosity of the films, suggesting that the transport through the TiO_2 material is not dominating the electric current. On the other hand, it can be seen from Figure 1 that capillary condensation becomes important above 60% RH in both mesoporous systems, namely, MT and MS, but the presence of water inside the pores is still significant for lower RH values.

DOI: 10.1021/acs.jpcc.5b09418
J. Phys. Chem. C 2015, 119, 28954−28960

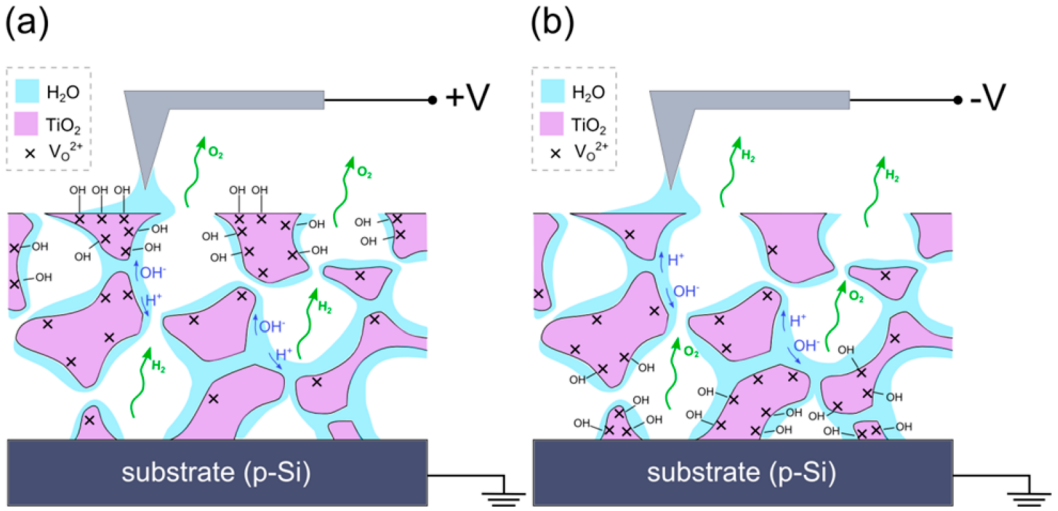

Figure 4. Schematics of the mechanism involved in the tip−sample system under positive (a) and negative (b) bias. Crosses indicate oxygen vacancies (V_O^{2+}), mostly formed when the TiO_2 is under electrical stress for either polarization. In both cases, the ionic products of water electrolysis (OH^-, H^+) contribute to a non purely electronic conduction, and some OH^- ions are adsorbed at oxygen vacancy sites. This latter process is enhanced at the surface for positive bias, thus contributing to the observed change in the topographic images (features in this illustration are not to scale).

However, for the MS case, no electric conduction was observed in the CAFM results at any RH. From this fact, we can assume that the current measured in high RH conditions for TiO_2 films should not arise simply by water electrolysis inside the pores between the CAFM tip and the silicon substrate.

The different RH regimes observed for the MT film seem to be related to the different structural phases of the water confined in the pores, as it is known that the interaction of water with TiO_2 surfaces is around three times stronger than SiO_2.[27] Using molecular dynamics simulations, in ref 27, the structure of the water confined in TiO_2 pores was studied as a function of the water filling fraction. The authors found that, before capillary condensation occurs, the water filling develops by forming a homogeneous water layer on the titania pore surface. From Figure 1, we can deduce that our experiments were carried out in the water layered phase for the highest RH conditions. Therefore, the increase of the conduction might be originated by the electrochemical reduction of the titania surface, which in turn favors a dissociation of water molecules, suggesting that the main electric transport mechanism in MT films is the titania-assisted water electrolysis at the TiO_2−water interface inside the pores. The mechanism involved in water−titania interactions has already been explored both experimentally and theoretically, demonstrating that defects associated with oxygen vacancies are active sites for water molecule dissociation and OH^- groups adsorption.[3,28,29]

The effects shown in Figures 2 and 3, which were not observed for the NMT in the same RH and bias voltage conditions, are enhanced and become measurable by combining the strong applied electric field at the AFM tip and the highly accessible titania pores surface. In the presence of an electric field, oxygen vacancies might be created at the surface due to electrochemical reactions[4,30] or migrate and redistribute through the oxide.[31−33] CAFM experiments on n-type TiO_2 samples display an increase of the electric resistance on the obtained patterns giving rise to field-assisted adsorption of oxygen molecules.[14,15] These articles propose that the scanned surface would be oxidized during the CAFM procedure. In other words, non stoichiometric titania would locally transform to the stoichiometric insulating state. Within this scenario, our results would suggest that the presence of oxygen vacancies at the initial state is very low in the MT films. Therefore, our films are majorly stoichiometric TiO_2, and most of the oxygen vacancies would be created by CAFM induced electrochemical reactions. Figure 4 schematizes the role of the electric polarization of the AFM tip for the mechanisms involved in the EL described.

When the tip is positively charged, oxygen ions are attracted becoming O_2 and consequently oxygen vacancies appear at the TiO_2 surface. The whole process is completed with the water electrolysis products (H^+, OH^-, O_2), generating ions that would contribute to a non purely electronic conduction (see Figure 4a). At the highest RH values, the adsorption of either OH^- or H_2O at the positively charged oxygen vacancies results in the modification of the topography observed in Figure 2c.[26] These results are in agreement with similar experiments reported on CeO_2 films by Yang et al.[10] where the topography is structurally modified due to protons being pulled away from the surface and into the bulk with the consequent hydroxide formation.

When the tip is negatively charged, the electrochemical process is similar, but the geometry of the system is reversed, and most oxygen vacancies would appear at the surfaces of the pores, which are closer to the substrate (see Figure 4b). In this case, far from an erasing effect, the change of polarity between successive scans would produce an accumulative decrease of the local resistance (as shown in Figure 3d). Thus, for negative bias voltages, the local electrical properties of the MT film are modified in the scanned area without any trace on the topography.

■ CONCLUSIONS

We have shown the local probing of electrochemically modified mesoporous TiO_2 thin films. Unlike usual SPM experiments, where the effects are localized on the upper surface, we were able to control the electric properties inside the volume of the film below the scanned area by exploiting the mesoporous structure. Our experiments strongly suggest that the effect

DOI: 10.1021/acs.jpcc.5b09418
J. Phys. Chem. C 2015, 119, 28954−28960

might develop at the water−TiO_2 interface inside the pores, where the whole process would result from the electrochemically reduced MT surface combined with titania-assisted water electrolysis. Thus, our results highlight the relevance of the structural characteristics of the TiO_2 films, directly related with the fabrication technique, and the effects of the environmental interactions at the titania surface on the electrical response of titania-based devices.

Furthermore, we demonstrated that in mesoporous TiO_2 thin films it is possible to modify the buried electrical conduction properties, either with or without changes on the topography, by simply adjusting the proper humidity and bias voltage conditions. Therefore, our findings could inspire novel nanofabrication methods through the development of electrochemical lithography techniques, with the additional advantage of working at ambient conditions.

■ ASSOCIATED CONTENT

Supporting Information

The Supporting Information is available free of charge on the ACS Publications website at DOI: 10.1021/acs.jpcc.5b09418.

(I) Structural characterization of the mesoporous films, (II) additional CAFM characterization of the MT films, (III) CAFM characterization of the NMT and MS films, and (IV) current−voltage characteristics of MT at the CAFM experiments (PDF)

■ AUTHOR INFORMATION

Corresponding Author

*E-mail: granja@tandar.cnea.gov.ar.

Notes

The authors declare no competing financial interest.

■ ACKNOWLEDGMENTS

The authors gratefully acknowledge financial support received from CONICET (PIP 00044CO, PIP00362), ANPCyT (PICT 2012-2087), UNSAM, and ABTLuS (for access to SAXS2−LNLS beamline). Dr. P. Bozzano and G. Zbihlei (CNEA) are thanked for the TEM images. L.P.G., M.C.F., V.F., P.L., and G.J.A.A.S. are CONICET staff members.

■ REFERENCES

(1) Chen, X.; Selloni, A. Titanium Dioxide Nanomaterials. *Chem. Rev.* **2014**, *114*, 9281−10216.

(2) Diebold, U. The Surface Science of Titanium Dioxide. *Surf. Sci. Rep.* **2003**, *48*, 53−229.

(3) Bikondoa, O.; Pang, C. L.; Ithnin, R.; Muryn, C. A.; Onishi, H.; Thornton, G. Direct Visualization of Defect-Mediated Dissociation of Water on TiO_2 (110). *Nat. Mater.* **2006**, *5*, 189−192.

(4) Szot, K.; Rogala, M.; Speier, W.; Klusek, Z.; Besmehn, A.; Waser, R. TiO_2 - a Prototypical Memristive Material. *Nanotechnology* **2011**, *22*, 254001−254022.

(5) Fuertes, M. C.; Barrera, M. P.; Plá, J. Sorption and Optical Properties of Sol-Gel Thin Films Measured by X-Ray Reflectometry and Ellipsometric Porosimetry. *Thin Solid Films* **2012**, *520*, 4853−4862.

(6) Dimitrov, D. B.; Koprinarova, J.; Pazov, J.; Angelov, Ch. Conductivity of Micro-Porous Magnetron-Sputtered Thin TiO_2 Films. *Vacuum* **2000**, *58*, 344−350.

(7) García, R.; Martinez, R. V.; Martinez, J. Nano-Chemistry and Scanning Probe Nanolithographies. *Chem. Soc. Rev.* **2006**, *35*, 29−38.

(8) Weeks, B. L.; Vaughn, M. W.; DeYoreo, J. J. Direct Imaging of Meniscus Formation in Atomic Force Microscopy Using Environmental Scanning Electron Microscopy. *Langmuir* **2005**, *21*, 8096−8098.

(9) Simeone, F. C.; Albonetti, C.; Cavallini, M. Progress in Micro- and Nanopatterning via Electrochemical Lithography. *J. Phys. Chem. C* **2009**, *113*, 18987−18994.

(10) Yang, N.; Doria, S.; Kumar, A.; Jang, J. H.; Arruda, T. M.; Tebano, A.; Jesse, S.; Ivanov, I. N.; Baddorf, A. P.; Strelcov, E.; Licoccia, S.; Borisevich, A. Y.; Blestrino, G.; Kalinin, S. V. Water-mediated Electrochemical Nano-writing on Thin Ceria Films. *Nanotechnology* **2014**, *25*, 075701.

(11) Mathur, N.; Littlewood, P. Nanotechnology: The third way. *Nat. Mater.* **2004**, *3*, 207−209.

(12) Yurtsever, A.; Sugimoto, Y.; Abe, M.; Morita, S. NC-AFM Imaging of the TiO2 (110)-(1 × 1) Surface at Low Temperature. *Nanotechnology* **2010**, *21*, 165702−165709.

(13) Boxley, C. J.; White, H. S.; Gardner, C. E.; Macpherson, J. V. Nanoscale Imaging of the Electronic Conductivity of the Native Oxide Film on Titanium Using Conducting Atomic Force Microscopy. *J. Phys. Chem. B* **2003**, *107*, 9677−9680.

(14) Kim, Y.; Jang, J. H.; Park, S.-J.; Jesse, S.; Donovan, L.; Borisevich, A. Y.; Lee, W.; Kalinin, S. V. Local Probing of Electrochemically Induced Negative Differential Resistance in TiO_2 Memristive Materials. *Nanotechnology* **2013**, *24*, 085702−085710.

(15) Kobayashi, K.; Tomita, Y.; Yoshida, S. Nanometer-Scale Patterning of Oxygen Molecules Adsorbed on TiO_2 Surface by an Atomic Force Microscope with a Conductive Cantilever. *Nano Lett.* **2002**, *2*, 925−927.

(16) Brinker, C. J.; Lu, Y.; Sellinger, A.; Fan, H. Evaporation-Induced Self-Assembly: Nanostructures Made Easy. *Adv. Mater.* **1999**, *11*, 579−585.

(17) Innocenzi, P.; Malfatti, L. Mesoporous Thin Films: Properties and Applications. *Chem. Soc. Rev.* **2013**, *42*, 4198−4216.

(18) Soler-Illia, G. J. A. A.; Angelomé, P. C.; Fuertes, M. C.; Calvo, A.; Wolosiuk, A.; Zelcer, A.; Bellino, M. G.; Martínez, E. D. Mesoporous Hybrid and Nanocomposite Thin Films. A Sol-Gel Toolbox to Create Nanoconfined Systems with Localized Chemical Properties. *J. Sol-Gel Sci. Technol.* **2011**, *57*, 299−312.

(19) Soler-Illia, G.; Angelome, P. C.; Fuertes, M. C.; Grosso, D.; Boissiere, C. Critical Aspects in the Production of Periodically Ordered Mesoporous Titania Thin Films. *Nanoscale* **2012**, *4*, 2549−2566.

(20) Angelomé, P. C.; Fuertes, M. C.; Soler-Illia, G. J. A. A. Multifunctional, Multilayer, Multiscale: Integrative Synthesis of Complex Macro and Mesoporous Thin Films with Spatial Separation of Porosity and Function. *Adv. Mater.* **2006**, *18*, 2397−2402.

(21) Crepaldi, E. L.; Soler-Illia, G.J. de A. A.; Grosso, D.; Cagnol, F.; Ribot, F.; Sanchez, C. Controlled Formation of Highly Organized Mesoporous Titania Thin Films: From Mesostructured Hybrids to Mesoporous Nanoanatase TiO_2. *J. Am. Chem. Soc.* **2003**, *125*, 9770−9786.

(22) Soler-Illia, G. J. A. A.; Angelome, P. C.; Cecilia Fuertes, M.; Grosso, D.; Boissiere, C. Critical Aspects in the Production of Periodically Ordered Mesoporous Titania Thin Films. *Nanoscale* **2012**, *4*, 2549.

(23) Baklanov, M. R.; Mogilnikov, K. P.; Polovinkin, V. G.; Dultsev, F. N. Determination of Pore Size Distribution in Thin Films by Ellipsometric Porosimetry. *J. Vac. Sci. Technol., B: Microelectron. Process. Phenom.* **2000**, *18*, 1385−1391.

(24) Boissiere, C.; Grosso, D.; Lepoutre, S.; Nicole, L.; Bruneau, A. B.; Sanchez, C. Porosity and Mechanical Properties of Mesoporous Thin Films Assessed by Environmental Ellipsometric Porosimetry. *Langmuir* **2005**, *21*, 12362−12371.

(25) Martínez, E. D.; Granja, L.; Bellino, M. G.; Soler-Illia, G. J. A. A. Electrical Conductivity in Patterned Silver−Mesoporous Titania Nanocomposite Thin Films: Towards Robust 3D Nano-Electrodes. *Phys. Chem. Chem. Phys.* **2010**, *12*, 14445−14448.

(26) Yang, J. J.; Borghetti, J.; Murphy, D.; Stewart, D. R.; Williams, R. S. A Family of Electronically Reconfigurable Nanodevices. *Adv. Mater.* **2009**, *21*, 3754−3758.

DOI: 10.1021/acs.jpcc.5b09418
J. Phys. Chem. C 2015, 119, 28954−28960

(27) Gonzalez Solveyra, E.; de la Llave, E.; Molinero, V.; Soler-Illia, G.; Scherlis, D. A. Structure, Dynamics and Phase Behavior of Water in TiO_2 Nanopores. *J. Phys. Chem. C* **2013**, *117*, 3330−3342.
(28) Schaub, R.; Thostrup, P.; Lopez, N.; Lægsgaard, E.; Stensgaard, I.; Nørskov, J.; Besenbacher, F. Oxygen Vacancies as Active Sites for Water Dissociation on Rutile TiO_2 (110). *Phys. Rev. Lett.* **2001**, *87*, 266104.
(29) He, Y.; Tilocca, A.; Dulub, O.; Selloni, A.; Diebold, U. Local Ordering and Electronic Signatures of Submonolayer Water on Anatase TiO_2 (101). *Nat. Mater.* **2009**, *8*, 585−589.
(30) Yang, J. J.; Miao, F.; Pickett, M. D.; Ohlberg, A. A.; Stewart, D. R.; Lau, C. N.; Williams, R. S. The Mechanism of Electroforming of Metal Oxide Memristive Switches. *Nanotechnology* **2009**, *20*, 215201.
(31) Kwon, J.; Sharma, A. A.; Bain, J. A.; Picard, Y. N.; Skowronski, M. Oxygen Vacancy Creation, Drift, and Aggregation in TiO_2-Based Resistive Switches at Low Temperature and Voltage. *Adv. Funct. Mater.* **2015**, *25*, 2876−2883.
(32) Setvin, M.; Schmid, M.; Diebold, U. Aggregation and Electronically Induced Migration of Oxygen Vacancies in TiO_2 Anatase. *Phys. Rev. B: Condens. Matter Mater. Phys.* **2015**, *91*, 195403.
(33) Kwon, D.; Kim, K. M.; Jang, J. H.; Jeon, J. M.; Lee, M. H.; Kim, G. H.; Li, X. S.; Park, G. S.; Lee, B.; Han, S.; Kim, M.; Hwang, C. S. Atomic Structure of Conducting Nanofilaments in TiO_2 Resistive Switching Memory. *Nat. Nanotechnol.* **2010**, *5*, 148−153.

DOI: 10.1021/acs.jpcc.5b09418
J. Phys. Chem. C 2015, 119, 28954−28960